

Stability of the B=2 hedgehog in the Skyrme model

Thomas Waindzoeh*

Institut für Kernphysik, Forschungszentrum Jülich GmbH.

D-52425 Jülich, Germany

Jochen Wambach

University of Illinois at Urbana-Champaign

Department of Physics, Loomis Laboratory

1110 W.Green Street, Urbana IL 61801, USA

November 14, 2017

Abstract

We study the unstable modes of the baryon number two hedgehog of the Skyrme model on a three dimensional spatial lattice. An expansion of the Skyrme Lagrangian around the hedgehog configuration provides the equations of motion for the fluctuation fields solvable numerically via a relaxation method. We find the negative energy modes and, by evolving the excited hedgehog in time, a breakup into two separated solitonic configurations is obtained. Different paths of descent for the receding Skyrmions are presented and the possibility of determining the metric structure of the collective-coordinate manifold is discussed.

1 Introduction

The Skyrme model [1], as a semiclassical model of *QCD* in the non-perturbative regime, is quite successful in describing low-energy hadronic physics. Starting from a classical topological Skyrmion solution, the calculated single-baryon properties are in qualitative agreement with measured physical values. This is, in view of the few parameters of the model, quite remarkable. A challenging problem is to apply the model to more than one baryon and to study the interaction of baryons within the picture of interacting Skyrmions. Due to the non-linear structure of the model, the equations of motion for

*electronic address: T.Waindzoeh@kfa-juelich.de

more than one Skyrmion are very hard to solve and usually one avoids this difficulty by constructing the multi-Skyrmion configuration out of the known single fields. However, the often used 'product ansatz' in the two-Skyrmion case, valid for large separation, cannot reproduce the axially symmetric minimal energy configuration and therefore fails to give any medium-range attraction in the central component of the nucleon-nucleon interaction. This medium-range attraction was found only after performing a full lattice calculation [2, 3, 4]. This tells us, that one should not rely on approximations for short distances of the Skyrmions. They interact strongly and one has to know the exact field configuration in order to make valid statements about the physics.

Although some features of the nucleon-nucleon interaction were obtained within the Skyrme model, many parts of the potential are still unresolved or missing. As a consequence, the phase shifts for the interaction are described fairly inaccurately [5]. This insufficient result is mostly due the lack of knowledge on the short-distance behavior of the Skyrmion dynamics. This dynamics contains the necessary information for the semiclassical quantization of the model and a detailed understanding of the different properties of interacting Skyrmions becomes very important. The Skyrmion-Skyrmion interaction potential has been calculated previously [6, 7], but contributions from the inertia tensor of the Skyrmions remain largely unknown. The momentum operators in the collective-coordinate quantization scheme are connected to this inertia tensor and any description will be incomplete as long as the Hamiltonian misses proper kinetic energy terms. The investigation of the explicit form of the inertia tensor and its dependence on the separation of the two Skyrmions will therefore be the main purpose of the present study.

To gain more insight into the short-distance properties of the two-Skyrmion sector, we analyze the stability of the $B=2$ hedgehog on a three dimensional spatial lattice. This special Skyrmion configuration is important because it can serve as an starting point for obtaining many different two-Skyrmion configurations at finite separation [8]. The hedgehog is a saddle point in the energy surface and thus unstable to certain excitations. Since the Skyrmions carry a conserved topological number, the decay path starting from the excited hedgehog will connect different Skyrmion configurations in the same topological sector. Following various paths one should be able to construct the full Skyrmion-Skyrmion interaction potential and the inertia tensor from the given information.

In this paper we wish to perform the first part of this program, namely the calculation of the decay paths for the $B=2$ hedgehog. Therefore the paper is organized as follows: in the next section we briefly introduce the Skyrme model Lagrangian and discuss the collective-coordinate Hamiltonian for the baryon number $B=2$ sector. After presenting the numerical method, we will investigate the stability of the $B=2$ hedgehog and explicitly calculate its unstable modes on the lattice. By evolving the fields in

time, we obtain different paths of descent from the hedgehog and we will discuss the connection to the collective-coordinate description. Conclusions and a short outlook on future work will end the paper.

2 The Skyrme model

2.1 The Lagrange density

The Skyrme model is an effective chiral theory to model QCD in the non-perturbative regime. For large values of N_C , the number of colors for quarks and gluons, t'Hooft [9] and later on Witten [10] showed, that QCD reduces to a theory of weakly interacting mesons (and glue balls) where the baryons emerge as solitonic solutions of the classical field equations. This large- N_C expansion, unfortunately, has never been worked out systematically due to enormous algebraic and technical problems for 3+1 dimensions. Hence one has to study models, which attempt to capture the main features of large- N_C QCD . These models should obey the known low-energy theorems for meson physics dictated by chiral symmetry and current algebra. One of the simplest models, which fulfills this requirement, is the Skyrme model. It is widely believed, that it represents the essential parts of the true large- N_C expansion, if it ever will be developed from QCD .

The Lagrange density of the Skyrme model can be written as [1]

$$\mathcal{L} = \frac{f_\pi^2}{4} \text{Tr}[\partial_\mu U \partial^\mu U] + \frac{1}{32e_s^2} \text{Tr}([U^\dagger \partial_\mu U, U^\dagger \partial_\nu U])^2 + \frac{m_\pi^2 f_\pi^2}{2} \text{Tr}[U - 1] , \quad (1)$$

where the non-linear pion field U is a unitary $SU(2)$ matrix, obeying the chiral constraint

$$UU^\dagger = 1 . \quad (2)$$

A possible parameterization of U is of the form

$$U = (\sigma + i\vec{\tau}\vec{\pi})/f_\pi . \quad (3)$$

This shows the connection of the model to an effective meson theory for pions. The sigma field is not a free field, but depends on the pion field via the unitarity relation (2). The parameters of the model are the pion decay constant f_π , the physical pion mass m_π and the 'Skyrme parameter' e_s .

In addition to the description of low-energy pion interactions, the model simultaneously allows for baryons. Due to the fourth-order Skyrme term, which has the right number of spatial derivatives to obtain localized configurations in space, the field U

can be excited as a soliton, stabilized by topology. These special excitations, called Skyrmions, are characterized by a topological current

$$B^\mu = \frac{1}{24\pi^2} \epsilon^{\mu\nu\rho\sigma} \text{Tr}[(U^\dagger \partial_\nu U)(U^\dagger \partial_\rho U)(U^\dagger \partial_\sigma U)] , \quad (4)$$

which can be derived from the mapping properties of the fields. The time component of this current lead to a conserved topological quantity

$$B = \int d^3x B^0 = n , \quad (5)$$

representing the winding number of the field U . Physically this number can be identified with the baryon number [10].

For the topological sector with baryon number $B=1$, the description of the physical particles like the nucleon or the Δ -isobar is in qualitative agreement to experiment. For a detailed discussion of this sector see [11].

2.2 The $B=2$ sector of the model

The Skyrmion sector with the topological number $B=2$ is the domain where one studies the deuteron properties and the nucleon-nucleon interaction. Different solitonic configurations are known for $B=2$ and some of them have been studied previously [12, 2, 4]. All classical configurations are characterized by a set of coordinates which transform one configuration into an other. In the semiclassical quantization scheme, these coordinates become operators and allow for the description of the physical particles.

To perform realistic calculations within the model, however, one should truncate the set of coordinates from the beginning. Comparing the energy shifts of the Skyrmion, one can group the corresponding transformations into two essentially different sets. Vibrations arising from explicit pionic excitations of the solitonic background field are of relatively high energy compared with the zero- or nearly zero modes for a given configuration. One should treat these vibrations via perturbation theory and, to first order, simply neglect them. It remains a problem left for future studies to consider explicitly the vibrational modes of the Skyrmions in order to perform the renormalization program. Most important for a first description of the physical processes are the zero- or nearly zero modes. To first order in a perturbation theory of semiclassical quantization, these modes cannot be neglected in the baryonic sector.

Going back to the work of Manton [8] on the $B=2$ sector the minimal number of coordinates for the description of the Skyrmion-Skyrmion dynamics is twelve. In general there are three coordinates for global translations, three for spatial rotations and three

for isorotations. The corresponding transformations are related to the symmetries of the field U and define true zero modes. The remaining three coordinates describe the orientation of two individual $B=1$ Skyrmions relative to each other. This orientation is determined by one coordinate for the relative separation and two angles for the relative isospin rotation. These relative coordinates are connected to modes, which change the energy. The energy shift is rather small, however, compared to the total field energy at least for large distances. For example is the energy difference between the 'donut', which is the axially-symmetric solution to minimal energy, and two infinitely separated Skyrmions only a few percent of the total mass of the donut. This means, that one should treat these coordinates like the zero modes in the collective-coordinate approach. They cannot be neglected like the vibrations.

In the collective coordinate approach, the U -field will have the form

$$U(x, t) = A(t)U(D(B(t))x - R_t(t), R(t), C(t))A^\dagger(t) , \quad (6)$$

where the time dependence is shifted to the coordinates R_T, B, A, R and C , which represent the three translations, three rotations, three isorotations, the relative separation and the relative isorotation respectively. The relative coordinates are internal coordinates of the field since they change explicitly the form and the energy of the soliton. Using this ansatz one arrives at the following classical collective-coordinate Hamiltonian for the $B=2$ sector of the Skyrme model

$$H = \frac{1}{2}P_i M_{ij}^{-1}(R, C)P_j + U(R, C) + 2M_H . \quad (7)$$

Here $P_i = M_{i,j}(R, C)\dot{Q}_j$ are the canonical momenta conjugate to the coordinates

$$Q_i = (A, B, R_T, R, C) . \quad (8)$$

The Skyrmion-Skyrmion interaction potential $U(R, C)$ and the mass matrix $M_{ij}(R, C)$ are functions of the relative coordinates R and C . For quantization, the collective coordinates and their momenta are replaced by operators which fulfill the canonical commutation relations

$$[\hat{P}_i, \hat{Q}_j] = i\delta_{ij} . \quad (9)$$

This will lead to a quantum Hamiltonian for the $B=2$ sector capable of describing the low-energy interaction of two baryons.

Before one can go over to the study of physical processes one first has to reliably determine the entries of the classical Hamiltonian. The interaction potential $U(R, C)$ has been determined previously on a spatial lattice [13]. One is then left with the

evaluation of the mass matrix $M_{ij}(R, C)$. One method is to use the explicit dependence of the fields on the collective coordinates. This leads to the expression

$$M_{ij}(R, C) = \int d^3x \frac{\partial \phi_\alpha}{\partial Q_i} M_{\alpha\beta} \frac{\partial \phi_\beta}{\partial Q_j} \quad (10)$$

where $M_{\alpha\beta}$ is the metric of the Skyrme model Lagrangian. Its form is given in (19). Since the B=2 configurations are changing under the relative transformations, it implies that one has to calculate the fields at many different points (R, C) in order to determine the field derivatives to the coordinates Q_i . This is very tedious and some results will be presented in a forthcoming paper [14].

Alternatively, one can perform time-dependent simulations of the dynamics. Starting from some initial condition, the solitonic motion can be followed numerically and by comparing the results with paths from the collective coordinate Hamiltonian (7) one should be able to deduce the structure of the mass matrix. In terms of the collective coordinates, the equations of motion for the time evolution are of the form

$$M_{ij}(R, C)\ddot{Q}_j + \Gamma_{ijk}^{(1)}(R, C)\dot{Q}_j\dot{Q}_k = -\frac{\partial U(R, C)}{\partial Q_i} \quad (11)$$

where the Christoffel symbols of the first kind are

$$\Gamma_{ijk}^{(1)}(R, C) = \frac{1}{2} \left[\frac{\partial M_{ij}(R, C)}{\partial Q_k} + \frac{\partial M_{ik}(R, C)}{\partial Q_j} - \frac{\partial M_{jk}(R, C)}{\partial Q_i} \right]. \quad (12)$$

If the collective-coordinate picture is valid, these equations of motion should describe the motion of the soliton fields and therefore be directly comparable to numerical lattice results. By calculating the relative coordinates and the potentials for a given path $\Gamma = (R, C)$ in the simulation one could therefore determine the mass matrix. In the following we will see to what degree this will be possible. Since our interest is in the short-distance dynamics of the two-Skyrmion system we will start from an initial B=2 hedgehog.

3 The numerical method

Before studying the stability of the B=2 hedgehog on the lattice we wish to discuss the numerical method used in this paper. To perform calculations for the field U on a three-dimensional lattice we switch to the parameterization

$$U = \phi_0 + i\vec{\tau}\vec{\phi}, \quad (13)$$

where the four fields ϕ_α are now constrained to lie on the unit chiral circle

$$\phi_\alpha^2 = 1. \quad (14)$$

Here the greek indices run from 0 to 3 while the latin indices run from 1 to 3. The constraint has to be fixed via a Lagrange multiplier λ such that the Lagrange density becomes

$$\begin{aligned}\mathcal{L} = & \frac{f_\pi^2}{2}(\partial_\mu\phi_\alpha)^2 - \frac{1}{4e_s^2}(\partial_\mu\phi_\alpha)^2(\partial_\nu\phi_\beta)^2 + \frac{1}{4e_s^2}(\partial_\mu\phi_\alpha\partial_\mu\phi_\beta)^2 \\ & + m_\pi^2 f_\pi^2(\phi_0 - 1) + \frac{1}{2}\lambda(\phi_\alpha^2 - 1) .\end{aligned}\quad (15)$$

Since we are interested here in the classical dynamics the Euler-Lagrange equations for the fields ϕ_α

$$\partial_\mu \frac{\delta\mathcal{L}}{\delta\partial_\mu\phi_\alpha} - \frac{\delta\mathcal{L}}{\delta\phi_\alpha} = 0 \quad (16)$$

have to be solved. Using the canonical momenta $\pi_\alpha = \frac{\delta\mathcal{L}}{\delta\partial_t\phi_\alpha}$ to the fields ϕ_α , one obtains a set of coupled non-linear partial differential equations

$$\partial_t\phi_\alpha = M_{\alpha\beta}^{-1}\pi_\beta , \quad (17)$$

$$\partial_t\pi_\alpha = \partial_i(C_{\alpha\beta}\partial_i\phi_\beta) + m_\pi^2 f_\pi^2 \delta_{0\alpha} + \lambda\phi_\alpha . \quad (18)$$

The 4×4 matrices $M_{\alpha\beta}$ and $C_{\alpha\beta}$ are functionals of the fields and have the form

$$M_{\alpha\beta} = [f_\pi^2 + \frac{1}{e_s^2}(\partial_i\phi_\gamma)^2]\delta_{\alpha\beta} - \frac{1}{e_s^2}\partial_i\phi_\alpha\partial_i\phi_\beta , \quad (19)$$

$$C_{\alpha\beta} = [f_\pi^2 - \frac{1}{e_s^2}(\partial_\mu\phi_\gamma)^2]\delta_{\alpha\beta} + \frac{1}{e_s^2}\partial_\mu\phi_\alpha\partial_\mu\phi_\beta \quad (20)$$

where $M_{\alpha\beta}$ is the metric of the Skyrme model.

To solve these equations numerically a finite differencing scheme is employed. The fields and the momenta are defined on a cartesian lattice (i, j, k) and the spatial derivatives are evaluated via central differences as

$$\partial_x\phi_\alpha(i, j, k) = \frac{\phi_\alpha(i+1, j, k) - \phi_\alpha(i-1, j, k)}{2\Delta x} , \quad (21)$$

$$\partial_x^2\phi_\alpha(i, j, k) = \frac{\phi_\alpha(i+1, j, k) - 2\phi_\alpha(i, j, k) + \phi_\alpha(i-1, j, k)}{\Delta x^2} \quad (22)$$

and so on.

For the time evolution we use the Leapfrog method

$$\pi_\alpha^n = \pi_\alpha^{n-2} + 2\Delta t[\partial_i(C_{\alpha\beta}^{n-1}\partial_i\phi_\beta^{n-1}) + m_\pi^2 f_\pi^2 \delta_{0\alpha} + \lambda\phi_\alpha^{n-1}] , \quad (23)$$

$$\phi_\alpha^{n+1} = \phi_\alpha^{n-1} + 2\Delta t[(M_{\alpha\beta}^{-1})^n\pi_\beta^n] . \quad (24)$$

As initial conditions the fields have to be predetermined at the two time steps $t = -1, 0$ and the momenta at the time steps $t = -2, -1$. The fields and momenta on the lattice

boundary are set to their vacuum values. The Lagrange parameter λ is adjusted during the iteration process to ensure the chiral constraints $(\phi_\alpha^{n+1})^2 = 1$ and $\phi_\alpha^n \partial_t \phi_\alpha^n = 0$. The latter results from the time derivative of the first and both have to be satisfied simultaneously.

The Leapfrog method is easily adapted as a relaxation method for calculating static solutions to the field equations. Considering time as pseudotime, one performs the calculation of the momenta at pseudotime step t^n with vanishing momenta and time derivatives from previous pseudotime steps. This method advances the fields to a static configuration since the configuration loses more and more of its kinetic energy as pseudotime progresses.

In this paper the lattice is kept rather small in order to limit the amount of computational time. We take 42 points for each spatial direction with a grid distance of $\Delta x = 0.06 fm$. The physical volume of our 'cube' is thus $V = (2.8 fm)^3$. This size is large enough for a calculation of the unstable modes of the B=2 hedgehog but is certainly too small to simulate the time evolution as the hedgehog breaks up and individual Skyrmions emerge. For numerical stability we have to ensure the Courant-Levi condition

$$\frac{v\Delta t}{\Delta x} \ll 1, \quad (25)$$

where v is a velocity scale for the evolution of a given field configuration ($v \approx c$). Typically this ratio is around 0.1 in our calculations. There are, however, additional stability problems which will be discussed later in the paper.

The parameters of the Skyrme model are set to $f_\pi = 93 MeV$, $m_\pi = 138 MeV$ and $e_s = 4.76$. This choice ensures the correct strength of the asymptotic one-pion exchange potential for the nucleon-nucleon interaction within the model. However, the mass of a B=1 Skyrmion, $M_{B=1} = 1416 MeV$, turns out too large. This should be compared to the continuum limit of $M_{B=1} = 1463 MeV$. A lattice error of about 5% is tolerable for a first study.

4 Stability of the B=2 hedgehog on the lattice

4.1 The unstable manifold of Manton

In the language of geometry the mass matrix $M_{ij}(R, C)$ is nothing but the metric of the twelve dimensional collective-coordinate manifold for the B=2 sector. In contrast to interacting magnetic monopoles [15], the motion on this manifold is not geodesic due to the presence of the potential energy $U(R, C)$ (see eq. (11)). Following different

paths on the collective subspace of Skyrminion configurations one can thus draw conclusions to the geometrical and potential structure on the manifold. As a source of paths, Manton proposed to consider the B=2 hedgehog in more detail. This special configuration is not stable, but represents a saddle point in the energy plane. It has six different zero modes rather than nine for the most general B=2 configuration. The hedgehog symmetry simply connects space to isospin space and global rotations become equivalent to global isorotations, thus reducing the number of degrees of freedom by three. The B=2 hedgehog has also six unstable modes. This was already discussed by Manton and the modes were explicitly found later for the S^3 -sphere [16]. These modes lower the energy of the hedgehog and define the starting points for paths of steepest descent. Together with the zero modes one has, by superposition of unstable modes, a large number of available initial configurations to probe the manifold.

4.2 The B=2 hedgehog on the lattice

The hedgehog is determined by the ansatz

$$U(x) = \cos F(r) + i\vec{\tau}\hat{x} \sin F(r) \quad (26)$$

where the boundary conditions for the profile function $F(r)$ are chosen to ensure baryon number B=2:

$$F(0) = 2\pi, F(\infty) = 0. \quad (27)$$

One can easily obtain the profile function by minimizing the static energy for this ansatz numerically by solving the radial differential equation. For our parameter set we calculate the B=2 hedgehog mass as $M_2 = 4418 MeV$. This is nearly three times the B=1 hedgehog mass of $M_1 = 1463 MeV$.

For a numerical stability analysis of the B=2 hedgehog the continuum result is unsuited, however. Rather one has to start from the minimized lattice hedgehog. Thus we use the free hedgehog profile function to set up an initial configuration which is then relaxed via the procedure introduced above. To improve convergence we reduce the cube to one octant via boundary conditions given by the symmetries of the hedgehog ansatz. After several thousand iteration steps we obtain a lattice hedgehog mass of $M = 4118 MeV$ and a baryon number of $B = 1.83$. A comparison of the free profile functions with the extracted lattice profile function is shown in fig. 1.

To check the long-time stability of the lattice hedgehog we have evolved the fields in real time via the leapfrog method. Even after several thousand time steps no appreciable gain in kinetic energy has been detected.

The unstable modes of the hedgehog are modes of lower energy and are calculable from an expansion of the Lagrange density around the background fields ϕ_α^H . Inserting

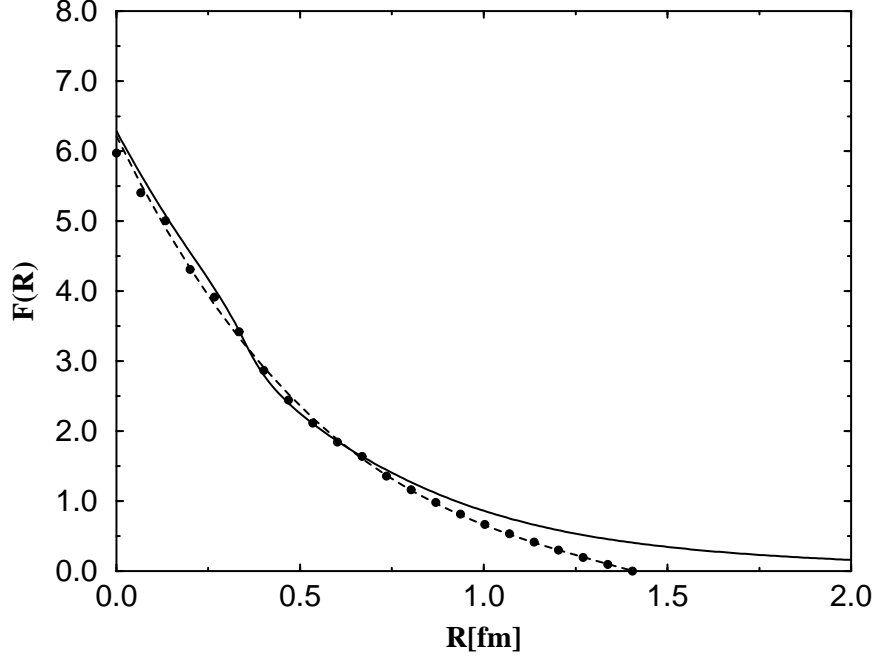


Fig. 1. The free (solid) and lattice (dots) profile function for the B=2 hedgehog.

the ansatz

$$\phi_\alpha = \phi_\alpha^H + \delta\phi_\alpha \quad (28)$$

into the Skyrme Lagrangian and keeping only terms up to second order in the small-amplitude fluctuations $\delta\phi_\alpha$, one obtains the expansion

$$\mathcal{L}[\phi] \approx \mathcal{L}[\phi^H] + \mathcal{L}^{(2)}[\phi^H, \delta\phi] . \quad (29)$$

Terms of first order in the fluctuations have to vanish due to the equations of motion for the extremal background field ϕ_α^H .

The explicit form of the second-order Lagrange density is

$$\mathcal{L}^{(2)}[\phi^H, \delta\phi] = \mathcal{T}^{(2)}[\phi^H, \delta\phi] - \mathcal{V}^{(2)}[\phi^H, \delta\phi] , \quad (30)$$

with the kinetic and potential energy densities given by

$$\mathcal{T}^{(2)}[\phi^H, \delta\phi] = \frac{1}{2}(\partial_t \delta\phi_\alpha) M_{\alpha\beta}[\phi^H] (\partial_t \delta\phi_\beta) , \quad (31)$$

$$\begin{aligned} \mathcal{V}^{(2)}[\phi^H, \delta\phi] = & \frac{f_\pi^2}{2}(\partial_i \delta\phi_\alpha)^2 + \frac{1}{2e_s^2}[(\partial_i \phi_\alpha)^2 (\partial_j \delta\phi_\beta)^2 + 2(\partial_i \phi_\alpha \partial_i \delta\phi_\alpha)(\partial_j \phi_\beta \partial_j \delta\phi_\beta) \\ & - (\partial_i \phi_\alpha \partial_i \phi_\beta)(\partial_j \delta\phi_\alpha \partial_j \delta\phi_\beta) - (\partial_i \phi_\alpha \partial_j \phi_\alpha)(\partial_i \delta\phi_\beta \partial_j \delta\phi_\beta) \\ & - (\partial_i \phi_\alpha \partial_j \delta\phi_\alpha)(\partial_j \phi_\beta \partial_i \delta\phi_\beta)] - \frac{1}{2}\lambda(\delta\phi_\alpha)^2 \end{aligned} \quad (32)$$

Here $M_{\alpha\beta}[\phi^H]$ again denotes the Skyrme model metric. The parameter λ ensures the chiral constraint and can be deduced from its equation of motion.

We use the leapfrog method for the second-order Lagrangian in order to determine the low-energy part of the mode spectrum. Starting from some initial fluctuation we relax the system to minimal energy

$$E^{(2)} = \int d^3x \mathcal{V}^{(2)}[\phi, \delta\phi] \quad (33)$$

until a stable solution $\delta\phi_\alpha(x)$ is found. During the iteration process we have to ensure the chiral constraint

$$\phi_\alpha^H \delta\phi_\alpha = 0 \quad (34)$$

via the usual Lagrange multiplier technique. The metric $M_{\alpha\beta}$ is used as an integration measure providing the normalization condition

$$\int d^3x \delta\phi_\alpha M_{\alpha\beta}[\phi^H] \delta\phi_\beta = \frac{1}{e_s^3 f_\pi} . \quad (35)$$

which normalizes the fluctuation fields to unity in dimensionless units.

Having found the first unstable mode, we then choose a new initial field and repeat the iteration scheme, while keeping the new field orthogonal (within the metric) to the previously determined fluctuation. In this way we can calculate a number of modes for a given background field. Unfortunately, our numerical method is only capable to determine locally stable configurations rather than absolute minima. We can easily miss some modes and the mode spectrum could be incomplete. However, a detailed analysis of the full spectrum is not the intention of this paper.

Following this scheme we have determined several negative-energy modes. Starting from an initial field configuration perpendicular to the hedgehog and with vanishing ϕ_0 component, the energy of the most unstable mode is found in our normalization to be

$$E_1^{(2)} = -12.3 MeV \quad (36)$$

The fluctuation field can be parameterized by a single function $g(r)$ and is of the form

$$\delta\phi_0 = 0 , \delta\phi_1 = -g(r)\hat{y} , \delta\phi_2 = g(r)\hat{x} , \delta\phi_3 = 0 . \quad (37)$$

Considering the spatial permutation symmetry of this solution one can obtain two other modes with the same energy. The degeneracy is therefore three. A comparison of the lattice fluctuation mode and the most unstable 'magnetic' mode on the S^3 -sphere, calculated by Wirzba et al. [16], is displayed in fig. 2.

Although the parameter set used by Wirzba et al. (vanishing pion mass) is slightly

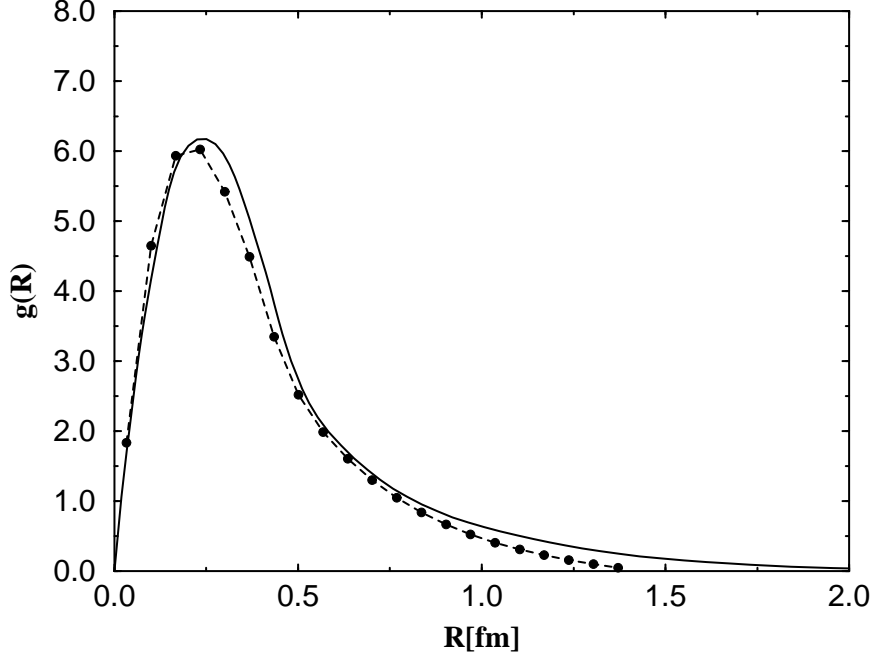


Fig. 2. The unstable 'magnetic' mode of the B=2 hedgehog. The solid line denotes the S^3 -sphere result for vanishing pion mass while the dots give the result for the lattice.

different to ours, the agreement is almost perfect. Assuming a sinusoidal time dependence for the fluctuation field, the fluctuation energy can also be expressed as imaginary frequency via the relation [16]

$$\omega_1^2 = (2e_s^3 f_\pi) E . \quad (38)$$

This yields $\omega_1 = -i497 MeV$, to be compared to the S^3 result of $\omega_m = -i460 MeV$.

The next higher-lying mode is found by choosing a non-vanishing zero component for the initial fluctuation field. After relaxation, we obtain the energy of the new field as

$$E_2^{(2)} = -6.4 MeV , \quad (39)$$

with a imaginary frequency of $\omega_2 = -i358 MeV$. This results can be compared with the 'electric' mode, the next unstable mode of the hedgehog on the S^3 -sphere with a frequency $\omega_e = -i260 MeV$. Since the comparison of the spatial form of the electric fields is almost as good as for the magnetic mode we believe that the major difference between the frequencies is due to lattice errors. The next higher (degenerate) mode found on the lattice has energy:

$$E_3^{(2)} = -1.9 MeV \quad (40)$$

and the spatial form is very close to the zero modes of the B=2 hedgehog in the continuum. A similar lattice analysis can be performed for the B=1 hedgehog. The lowest-energy mode is found to be

$$E_{B=1}^{(2)} = -0.7 MeV , \quad (41)$$

which is of the same order of magnitude (compared to the total hedgehog mass) as in the B=2 case. Since the B=1 hedgehog is absolutely stable, this fluctuation mode should be a true zero mode and indeed, by comparison, the form of the lattice fields is very similar to the continuum fields. Assuming that we can correct for lattice errors by shifting the entire spectrum such that the B=2 'zero mode' (40) has zero energy, we obtain

$$\omega_1 = -i457 MeV , \quad (42)$$

$$\omega_2 = -i300 MeV \quad (43)$$

for the two different unstable modes of the lattice hedgehog. These values are now very close to the S^3 -sphere results. The finite pion mass seems to have only minor influence on the B=2 hedgehog stability. To see, whether the calculated fluctuations really represent the unstable modes, we should look explicitly to the time evolution because imaginary frequencies imply exponential growth of the instability. This is studied in the next section.

5 The paths of descent for the B=2 hedgehog

5.1 The magnetic mode

With the calculated lattice fluctuation fields we can excite the B=2 hedgehog in a desired direction to run down the path of steepest descent. Via superposition of the background field with the calculated unstable modes and evolving the system in time we should find different splitting modes for the B=2 hedgehog. Starting first with the most unstable magnetic mode, a contour plot of the baryon number density at a fixed value of 0.2 and different time snapshots is shown in fig. 3. In the beginning the hedgehog hardly moves. The system is only very slowly responding to the fluctuation. After a certain amount of time, however, the configuration rapidly starts to stretch in one direction and finally splits into two – almost radially symmetric – B=1 Skyrmions. In analogy to nuclear physics this is the 'fission' mode for the B=2 hedgehog. A different view of the breakup process is given in fig. 4, where we have plotted the time evolution of a cut through the baryon number density along the direction of separation (the z axis).

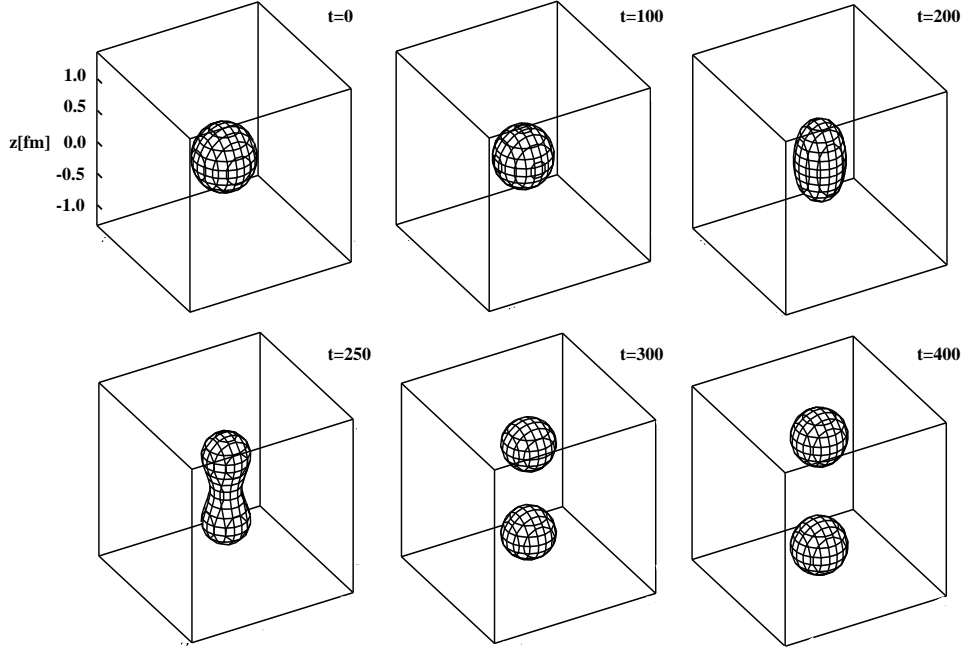


Fig. 3. The path of descent for different times (in units of the time step Δt) after excitation of the magnetic mode of the B=2 hedgehog. Shown is the contour plot of the baryon number density for the value $B^{(0)}(x) = 0.2$.

In order to numerically follow the path over long time periods we have to damp the motion along the path. Due to the high energy of the B=2 hedgehog configuration as compared to twice the B=1 hedgehog mass the outcoming Skyrmions carry more than 1GeV in kinetic and potential energy in addition to their rest masses. This energy, initially stored in the B=2 hedgehog, is gradually converted into deformation energy before it is released over a short time period in the fission process. At the fission point the kinetic energy density builds up rapidly and sharp peaks evolve which lead to a complete breakdown of the numerical method. The local field variations are simply too rapid to be correctly treated by the leapfrog method. However, the instability might have a deeper reason connected to a change of the characteristic of the Skyrme model equation of motion as discussed by Crutchfield et al. [17]. Due to the high kinetic energy of the fields at some points on the lattice the hyperbolic equation of motion could change into a non-hyperbolic differential equation. The latter type is very hard to control and is simply not tractable within our method. This problem needs much more advanced algorithms than we have at our disposal.

In order to cross the critical point we introduce an artificial viscosity in the equation of motion, as was done in the calculation of the scattering of two Skyrmions [18]. This

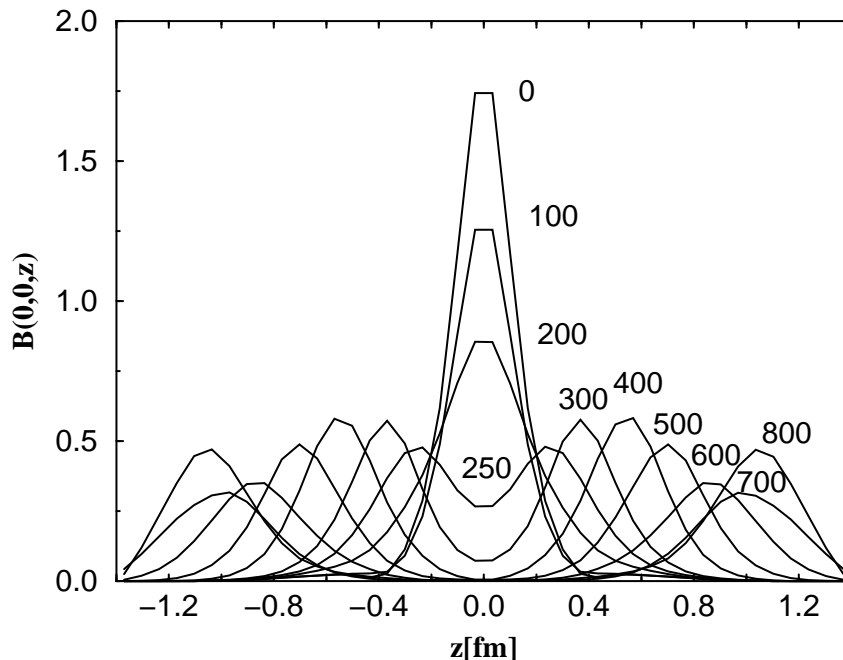


Fig. 4. The time evolution of a cut through the baryon number density along the z -axis (axis of separation).

viscosity dissipates kinetic energy, but it should not change the paths too drastically since it acts isotropically. To keep the influence on the dynamics minimal, the viscosity is turned on as late as possible and is switched off shortly after the critical point. Our numerical method remains stable, even with more than 700 MeV kinetic energy. This shows that only rapid local changes of the fields are critical, not large kinetic energies in general.

The total energy and the contributions from kinetic and potential energy for the fission mode is shown in fig. 5. Starting from zero kinetic energy, the $B=2$ solution gains very little kinetic energy in the beginning. Suddenly, the Skyrmons roll down the potential hill away from the $B=2$ hedgehog saddle and the full deformation energy of the hedgehog is transferred into kinetic energy of the receding Skyrmons. The viscous slow down leads to a decrease in total energy but, after the viscosity is turned off, the total energy remains almost constant. At that time an almost periodic exchange of potential and kinetic energy takes place partly hinting towards excitation of vibrational modes (see below). Such behavior has been observed previously in the numerical study of Skyrmon collisions [18].

In addition we have calculated the relative coordinates R and C as time progresses.

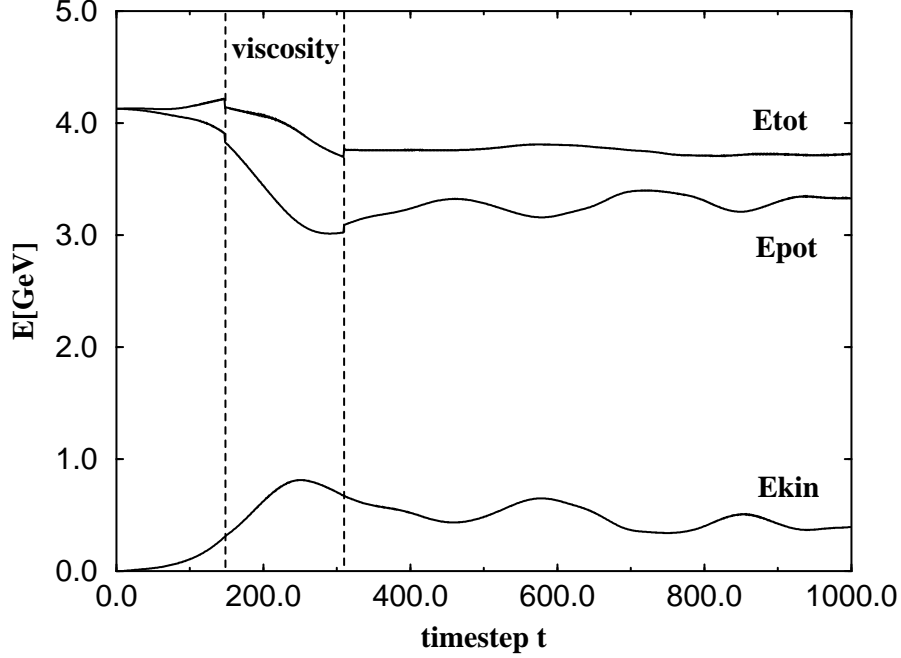


Fig. 5. The energies for the path of descent for the fission mode. The viscosity is turned on at times between the two dashed lines.

The relative separation is defined as the baryonic rms radius

$$R = \left(\int d^3x B^0(x) \vec{r}^2 \right)^{\frac{1}{2}} \quad (44)$$

while the relative isospin orientation can be determined via the symmetry relation

$$U(x, C) = C(\vec{\tau}\vec{n})U(D(i\vec{\tau}\vec{n})x, C)\vec{\tau}\vec{n}C^\dagger \quad (45)$$

where \vec{n} is a vector orthogonal to the axis of separation. Choosing the separation axis as the z-axis, relation (45) connects the fields for $z > 0$ to the fields at $z < 0$ and can be used to compute the relative isospin angles.

In fig. 6 the time dependence of both R and C , parameterized in the form

$$C = \cos \phi + i\tau_3 \sin \phi, \quad (46)$$

are given. The latter shows that the receding Skyrmions, which separate in the z-direction for this magnetic mode, rotate relative to each other around the separation axis. This rotation in isospin space can explain part of the periodic exchange of potential and kinetic energy, since the rotation in the relative coordinate space is connected to a energy shift of the Skyrmions. At late times the repulsive lattice boundary starts to become important. It slows down the Skyrmions and eventually scatters them back

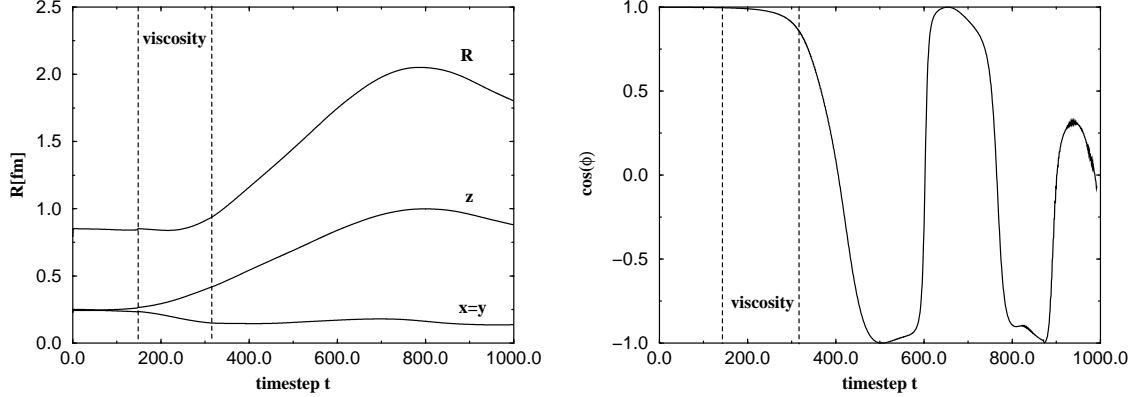


Fig. 6. The relative coordinates for the path of descent for the fission mode.

towards the center, as can be seen from the time dependence of R in the left part of fig. 6. To decrease the effect of the boundary and allow for undisturbed free motion of the two skyrmions at larger separations we would have to use a much larger lattice volume. The dominant part of the dynamics, however, arises in our opinion from the intrinsic deformation energies of the receding Skyrmions. In the beginning the gain in kinetic energy is only due to the new orientation of the fields to form the separated two single Skyrmions. The motion in relative coordinate space is there rather slow. Subsequently, as can best be seen in fig. 4, the single Skyrmions become strongly deformed. They exhibit a large compression shortly after the critical point and vibrate. This vibration is responsible for a considerable potential energy at large separation where one would expect a rather small potential energy from relative motion. The strong excitation of vibrational modes after the fission point implies that the collective-coordinate description in terms of zero and near zero modes along the path of descent is not well justified.

5.2 The electric mode

We have performed the same calculation for the less negative unstable mode which can be identified with the 'electric' mode of Wirzba et al. [16]. Also in this case viscosity has to be included to cross the critical point of the evolution. The critical point occurs at the same timestep as in the previous case. In order to visualize the breakup process for the 'electric' mode we display the baryon number density for two directions as a surface plot in fig. 7. Instead of splitting in the middle, the fields are now twisting outwards. This is understandable from the 'onion structure' of the baryon

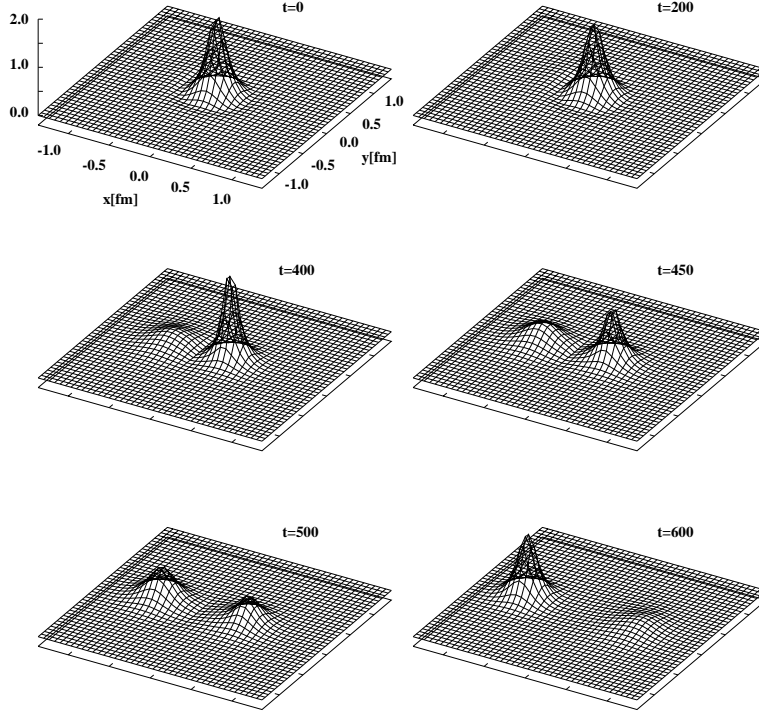


Fig. 7. The surface plot of the baryon number density for the 'twisting' mode.

density for the $B=2$ hedgehog. The density distribution is that of a single spherically symmetric $B=1$ Skyrmion around which a second Skyrmion is wrapped uniformly to cover the whole surface. The inner and outer Skyrmions are initially rotated relative to each other by the fluctuation field as can be determined by using the symmetry relation for the U -field (45). After the excitation, they start unwinding, inside out, which leads to a twist of the full baryon number density. The inner Skyrmion moves in one direction while the outer shell, also carrying baryon number one, recedes into the opposite direction. In addition, the solitons start rotating in space as well as in isospin space. While the spatial rotation can be determined we were not able to reliably calculate the isorotation due to lattice errors and the complicated nature of the motion. As compared to the magnetic (or fission) mode now two angles can vary. The calculated energies and the relative separation coordinate R for the magnetic path are shown in fig. 8. The results are qualitatively similar to the magnetic mode. Note however that it takes longer for the electric mode to start splitting since it is less unstable than the magnetic mode. The excitation of vibrational modes in the receding Skyrmions is even more pronounced, leading to very large amplitudes in the baryon number density, as it can be seen from fig. 7.

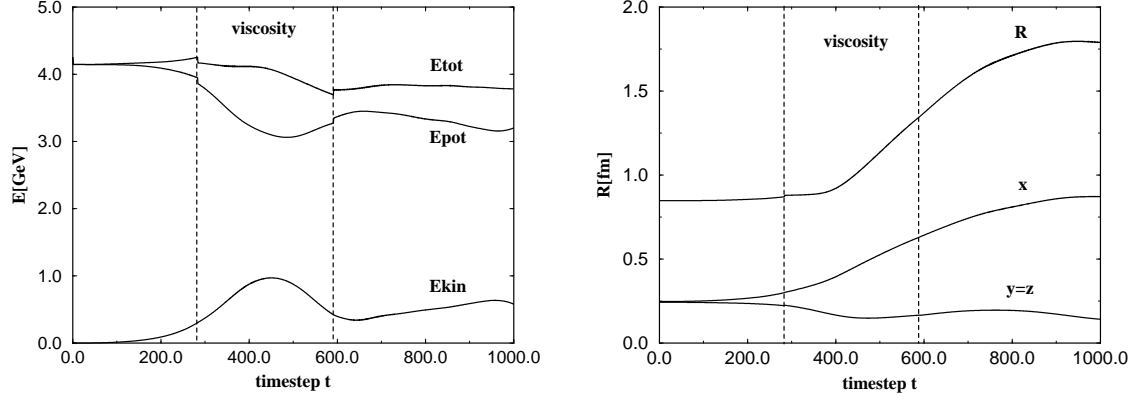


Fig. 8. The energies and cartesian coordinates of relative separation for the 'twisting' mode.

5.3 The path of steepest descent

The two paths studied in the previous sections have shown large excitations of vibrational modes for the separating $B=1$ Skyrmions. This is due to the fact that, by evolving the full system in time, we never really can follow the paths of steepest descent for the $B=2$ system. Only in the beginning of the iteration, when the energy is small, are we sure that the path will be close to the steepest one. For larger kinetic energies, however, we can easily leave this path and the analysis in terms of zero or near zero modes becomes exceedingly difficult due to the large number of vibrational modes.

To stay on paths of steepest descent, one can proceed in several ways. One method is to readjust for each superposition of background field and fluctuation the direction by calculating the new unstable mode for the full configuration (28). This precisely would define the path of steepest descent. The other method is to evolve the fields to a given time and then minimize the total energy at that instant of time by constraining the relative coordinates of the $B=2$ system. In this way one can get rid of internal excitations of the Skyrmions thus staying very close to the path of steepest descent. Probably this is the method to be used in the future.

With large viscous damping during the entire time evolution we can find paths, which should be close to some paths of steepest descent. One nice result is shown in fig. 9, where a combination of magnetic and electric mode as initial fluctuation field for the excitation of the $B=2$ hedgehog has been used. A specific mixture is necessary to orient the relative isospin such that the path ends up in the donut configuration. The existence of this path has been anticipated by Manton [8] and is confirmed by our calculations.

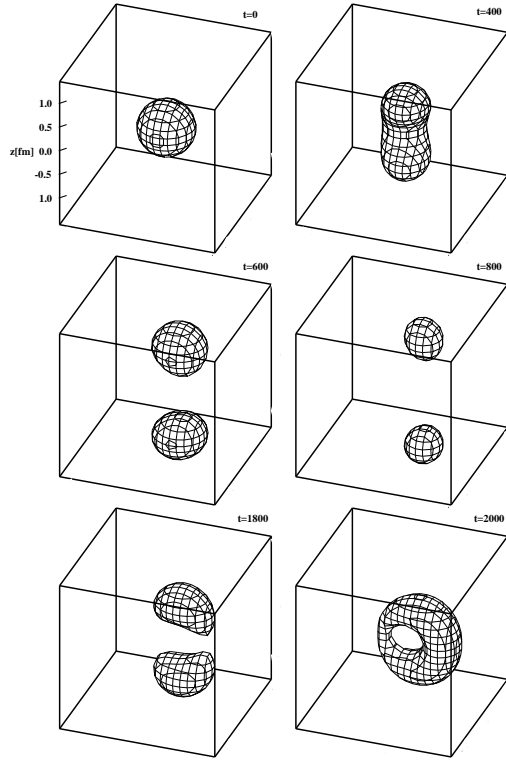


Fig. 9. Contour plot of the baryon number density for a fully slowed down path starting from an initial excitation of the B=2 hedgehog with a superposition of magnetic and electric modes.

6 Summary and Outlook

We have performed a stability analysis of the B=2 hedgehog on the lattice by solving the equations of motion for the fluctuation fields via relaxation employing the Leapfrog method in pseudotime. As conjectured by Manton [8] the hedgehog has six unstable modes, also on the lattice. Following the excited B=2 hedgehog in real time we find essentially two different decay pattern corresponding to two energetically different unstable and three-fold degenerate modes. One is the fission mode, where the baryon number density splits in the middle. This 'magnetic' mode has been found previously on the S^3 sphere [16]. The other type is the 'twister mode', where the inner B=1 Skyrmion of the B=2 hedgehog is twisting outwards from the full configuration. This mode is analogous to the 'electric' mode on the S^3 sphere [16]. Crossing the critical points of fission via viscous damping we see a complicated motion in space and isospace. Besides the relative motion, relevant for semiclassical quantization in terms of zero and near zero modes, the receding Skyrmions are excited vibrationally. The latter fact complicates the situation drastically. To avoid the excitation of vibrational modes one has to follow paths of steepest descent. As indicated in sect. 5.3 this could

be achieved by using a hybrid method of constrained static and free time-dependent lattice calculations. However, for this kind of method one has to constrain the fields for various orientations in order to calculate the metric of the collective coordinate manifold via the derivatives of the fields with respect to the coordinates (10). This is probably the only way to extract the inertia tensor of the B=2 Skyrminion system on the lattice.

Acknowledgments

We would like to thank Neil Snyderman for fruitful discussions. This work was supported in part by the grant NSF PHY94-21309. One of us (T.W.) acknowledges support from the German Academic Exchange Service (DAAD) under the program HSPII/AUFE.

References

- [1] T. H. R. Skyrme, Nucl. Phys. **31** (1962) 556.
- [2] J. J. M. Verbaarschot, T. S. Walhout, J. Wambach, and H. W. Wyld, Nucl. Phys. **A468** (1987) 520.
- [3] J. J. M. Verbaarschot, Phys. Lett **B195** (1987) 450.
- [4] V. B. Kopeliovich and B. E. Shtern, JETP Lett. **45** (1987) 203.
- [5] N. R. Walet, Phys. Rev. **C48** (1993) 2222.
- [6] T.S. Walhout and J. Wambach, Phys. Rev. Lett. **67** (1991) 314.
- [7] T. Wainzoch and J. Wambach, Phys. Lett. **B226** (1992) 163.
- [8] N.S. Manton, Phys. Rev. Lett. **60** (1988) 1916.
- [9] G. 't Hooft, Nucl. Phys. **B72** (1974) 461.
- [10] E. Witten, Nucl. Phys. **B160** (1979) 57.
- [11] G. Adkins, C. Nappi, and E. Witten, Nucl. Phys. **B228** (1983) 552.
- [12] M. Kutschera and C. J. Pethick, Nucl. Phys. **A440** (1985) 670.
- [13] T.S. Walhout and J. Wambach, Int. J. Mod. Phys. **E1** (1992) 665.
- [14] T. Wainzoch and J. Wambach, work in progress

- [15] G.W. Gibbons and N.S. Manton, Nucl. Phys. **B274** (1986) 183.
- [16] A. Wirzba and H. Bang, Nucl. Phys. **A515** (1990) 571.
- [17] W.Y. Crutchfield and J.B. Bell, J. Comp. Phys. **110** (1994) 234.
- [18] J. J. M. Verbaarschot, T. S. Walhout, J. Wambach, and H. W. Wyld, Nucl. Phys. **A461** (1987) 603.